An optimization method for the reduction of fertilization errors with centrifugal applicators

Jonas Koko, Teddy Virin

▶ **To cite this version:**

HAL Id: hal-00678112
https://hal.archives-ouvertes.fr/hal-00678112

Submitted on 12 Mar 2012

An optimization method for the reduction of fertilization errors with centrifugal applicators

Jonas KOKO[1] and Teddy VIRIN[2]

[1]LIMOS, Université Clermont 2 - CNRS UMR 6158 Campus des Cézeaux - BP 10125, 63173 Aubière, FRANCE, koko@isima.fr

[2]CEMAGREF Clermont-Ferrand, 03150 Montoldre, FRANCE, teddy.virin@cemagref.fr

Abstract

This paper discusses an optimization method for the spreading performed by centrifugal spreaders in order to minimize adverse environmental effects owing to application errors. A cost functional relying on a conventional simplified spread pattern model is proposed. In order to take into account the mechanical limits of the device, constraints are introduced. An augmented Lagrangian algorithm is implemented to compute an approximate solution. Numerical experiments show that application errors can be significantly reduced for parallel tracks within a main field body.

Keywords: Constrained nonlinear optimization, augmented Lagrangian, centrifugal spreaders.

1   Introduction

The fertilizer spreading consists in supplying nutrients within arable land in order to make up the soil deficiencies and thus permit a correct growth of the plants. According to the soil and crops characteristics, agricultural engineers state prescribed doses.These prescribed doses often take the form of dose maps. To get the distributed doses close to the prescribed ones, centrifugal spreaders with dual spinning discs are the most used. While the tractor progresses within the farmland along tramlines, fertilizer granulars contained in the hopper of the spreader pour onto each rotating disc and are ejected by centrifugal effect. The actual amount of applied fertilizers, usually called *spread pattern*, has an irregular distribution shape which is often highlighted by the transverse distribution curve calculated by summing the amounts along each travel direction.

Due to the spatial distribution heterogeneousness, the tractor equipped with the spreader follows outward and return paths in order to obtain a uniform deposit from transverse distributions summation for each successive travels. Thus, it is clear that transverse distributions play an important role in the fertilization strategy. Indeed, the device settings rely on their best arrangements according to the different tractor trajectories that is to say working widths. The working width is a concept widely used in the fertilization community and corresponds to the distance between two consecutive overlapping lines. Furthermore, when overlapping is optimal, these lines stand for symmetry axes and make two consecutive tracks coincide. Most of the experiments and simulations undertaken in order to assess fertilizer application accuracy or study device settings are only carried out by using this method to assess performance of applicators like in [1, 8, 12, 6] and advised for example by [11].

To reduce application errors, some works propose to find appropriate trajectories [5]. Unfortunately, this method is not suitable when tramlines are already settled by others agricultural practices like sowing. Therefore, it is important to know how best arrange the shape and the placement of the actual distributions (*i.e.* spread patterns) during spreading with respect to the prescribed geometrical constraints in the field. This adjustment should be continuously performed for each GPS position of the machine by changing its settings.

In this paper, we propose a new method for optimization of fertilizer application errors achieved during spreading. Instead of using the usual method based on the best arrangement of the transverse distribution advised by the different existing standards [1, 8], an optimization algorithm, based on a spread pattern model proposed by [3, 10], is used.

This paper is organized as follows. The next section deals with the mathematical modelling of the fertilizer application errors reduction problem. A space-time discretization is proposed in section 3. The optimization algorithm is then described in section 4. The section 5 illustrates numerical simulation results for parallel tramlines in a virtual field.

2   Mathematical modelling

Consider a polygonal two dimensional domain Ω and a time interval $(0, T)$. A generic point of Ω is denoted by x. Consider a rectilinear path $s(t) \in \Omega$, for all $t \in (0, T)$. For any point x in Ω, let $r(x, s(t))$ be the distance between $s(t)$ and x, and $\theta(x, s(t))$ the angle between the vector $\overrightarrow{s(t)x}$ and $s(t)$. In order to simplify notations, we will consider $r(x, t)$ and $\theta(x, t)$ instead of $r(x, s(t))$ and $\theta(x, s(t))$.

The spread pattern is currently defined by its medium radius and medium angle. The first parameter (varying with the speed of disc) corresponds to the distance between the

disc center and the spread pattern one, while the second (modifiable with the fertilizers dropping point on the disc) states the angle between the travel direction and the straight line passing through the disc center and the spatial distribution one.

Let us introduce the functions

- $\rho_1, \rho_2 : (0, T) \longrightarrow \mathbb{R}$, the medium radius of the left and right discs, respectively;
- $m_1, m_2 : (0, T) \longrightarrow \mathbb{R}$, the mass flow rates, at time t, of the left and right discs, respectively;
- $\varphi_1, \varphi_2 : (0, T) \longrightarrow \mathbb{R}$, the medium angle, at time t, of the left and right discs, respectively.

To simplify the notations, we set

$$m(t) = \begin{pmatrix} m_1(t) \\ m_2(t) \end{pmatrix}, \quad \rho(t) = \begin{pmatrix} \rho_1(t) \\ \rho_2(t) \end{pmatrix}, \quad \varphi(t) = \begin{pmatrix} \varphi_1(t) \\ \varphi_2(t) \end{pmatrix}$$

and

$$y(t) = \begin{pmatrix} m(t) \\ \rho(t) \\ \varphi(t) \end{pmatrix} \in \mathbb{R}^6, \quad \forall t \in [0,\ T].$$

According to Colin [3], the spatial distribution patterns for the right and left discs, at time t, are given by the functions $q_\alpha : \Omega \times (0, T) \longrightarrow \mathbb{R}$, $1 \le \alpha \le 2$, defined by

$$q_\alpha(x; y(t)) = \kappa m_\alpha(t) \cdot \exp \left(-\frac{(r(x,t) - \rho_\alpha(t))^2}{2\sigma_r^2} - \frac{(\theta(x,t) - \varphi_\alpha(t))^2}{2\sigma_\theta^2} \right), \qquad (2.1)$$

where

$$\kappa = \frac{1}{2\pi\sigma_r\sigma_\theta}. \qquad (2.2)$$

In (2.1) - (2.2), σ_r and σ_θ are known parameters and denote the standard deviation concerning for the medium radius and the medium angle at time t, respectively. The distribution pattern is then obtained by the function $q : \Omega \times (0, T) \longrightarrow \mathbb{R}$, defined by

$$q(x; y(t)) = \sum_{\alpha=1}^{2} q_\alpha(x; y(t)). \qquad (2.3)$$

From (2.3), the actual distributed dose $u(x, t)$ at time t is given by the function

$$u(x; y(t)) = \int_0^t q(x; y(\tau))d\tau, \quad \forall (x, t) \in \Omega \times (0, T). \qquad (2.4)$$

If we (reasonably) assume that $u(x; y(0)) = 0$, then the actual distributed dose (2.4) is the solution of the ordinary differential equation

$$\frac{\partial}{\partial t} u(x; y(t)) = q(x; y(t)), \quad \forall (x, t) \in \Omega \times (0, T), \qquad (2.5)$$

$$u(x, y(0)) = 0, \quad \forall x \in \Omega. \qquad (2.6)$$

Our goal is to minimize the application error at the end time T of the process, that is, the difference between the actual dose $u(x; y(T))$ and a prescribed dose u^*. That amounts to minimizing the L^2 error norm

$$E(y) = \frac{1}{2} \|u - u^*\|_{L^2(\Omega)}^2 = \frac{1}{2} \int_\Omega \left(u(x; y(T)) - u^*(x) \right)^2 dx. \qquad (2.7)$$

Since $y \mapsto q(x; y)$ is continuous, then u is a continuous function of y. The functional E is therefore continuous with respect to y.

In order to take into account the mechanical limits of the device, the functions m, ρ and φ and their time derivative must be subjected to bound constraints. It is reasonable to require that the unknown parameters m, ρ and φ be at least continuous functions. Let $\mathscr{C}^0(0, T)$ be the vector space of continuous functions and $\mathscr{C}^{0,1}(0, T)$ the space of Lipschitz functions on $(0, T)$. We define the set of admissible functions $\mathscr{K}$ by

$$\mathscr{K} = \left\{ y \in (\mathscr{C}^{0,1}(0, T))^6, \ |y_\ell(t)| \le a_\ell, \ |y'_\ell(t)| \le b_\ell, \ \ell = 1, \ldots, 6 \right\}, \tag{2.8}$$

where a_ℓ and b_ℓ are given positive constants chosen such a way that $\mathscr{K}$ is non-empty. The set of admissible functions $\mathscr{K}$ is a compact subset of the space of continuous functions $(\mathscr{C}^0(0, T))^6$. The problem of the reduction of fertilization errors now reads

Find $y^* \in \mathscr{K}$ such that :

$$E(y^*) \le E(y), \quad \forall y \in \mathscr{K}. \tag{2.9}$$

Remark 1. Since E is continuous and the set of admissible parameters $\mathscr{K}$ is compact, the optimization problem has at least one solution in $(\mathscr{C}^0(0, T))^6$.

Remark 2. In practice, sharp bounds can be used, i.e. $|y_\ell(t)| \le a_\ell$ can be replaced by $\underline{a}_\ell \le y_\ell(t) \le \overline{a}_\ell, \ \ell = 1, \ldots, 6$.

Remark 3. In most cases, there exist several tramlines and the actual distributed dose for all trajectories is then obtained by the summation of the applied dose q^k for each k-indexed path

$$u(x; y(t)) = \sum_{k=1}^{n_p} \int_0^t q^k(x; y(\tau)) d\tau \tag{2.10}$$

where n_p is the number of paths.

3 Numerical approximation

In practice, the problem (2.9) is approximated by a finite dimensional problem through a space-time discretization.

3.1 Finite dimensional optimization problem

The time discretization is performed by dividing the interval $(0, T)$ into n subintervals of equal length $\delta = T/n$. We set $t_i = i\delta$, $y^i = y(t_i)$ and

$$\boldsymbol{y} = \begin{pmatrix} y^0 \\ y^1 \\ \vdots \\ y^n \end{pmatrix}.$$

By using the trapezoidal rule in (2.4), the actual distributed dose map at the end time $u^n(x) := u(x; y(T))$ is approximated by

$$u^n(x) = \frac{\delta}{2} q(x; y^0) + \delta \sum_{i=1}^{n-1} q(x; y^i) + \frac{\delta}{2} q(x; y^n). \tag{3.1}$$

The cost functional (2.7) becomes

$$E_\delta(\boldsymbol{y}) = \frac{1}{2} \int_\Omega (u^n(x) - u^*(x))^2 \, dx \tag{3.2}$$

We assume that the polygonal domain Ω can be entirely gridded into quadrilaterals (i.e. parallelograms) Ω_e with

$$\bar\Omega = \bigcup_{e=1}^{P_h} \Omega_e,$$

where $h > 0$ is a size parameter. We also assume that u^n can be approximated, on a parallelogram Ω_e, by a bilinear polynomial u_h^n. Then the cost functional becomes

$$E_{\delta h}(\boldsymbol{y}) = \frac{1}{2} \sum_{e=1}^{P_h} \int_{\Omega_e} (u_h^n(x) - u^*(x))^2 \, dx. \tag{3.3}$$

The integral over a parallelogram can now be computed by a quadrature formula. Let $\{x_e^j\}_{i=1,\dots,4}$ be the vertices of a parallelogram Ω_e. Then element integral in (3.3) can be approximated by

$$\int_{\Omega_e} (u_h^n(x) - u^*(x))^2 \, dx \approx \frac{|\Omega_e|}{4} \sum_{j=1}^{4} \left(u_h^n(x_e^j) - u^*(x_e^j) \right)^2 \tag{3.4}$$

where $|\Omega_e|$ is the area of the parallelogram Ω_e. From (3.3) and (3.4), it follows that the finite dimensional cost functional is

$$E_{\delta h}(\boldsymbol{y}) = \frac{1}{8} \sum_{e=1}^{P_h} \sum_{j=1}^{4} |\Omega_e| \left(u_h^n(x_e^j) - u^*(x_e^j) \right)^2. \tag{3.5}$$

By using the trapezoidal rule (3.1), we have implicitly assumed a linear approximation of y. Then, the set of admissible functions (2.8) is approximated by the following finite dimensional subset

$$\mathcal{K}_\delta = \left\{ \boldsymbol{y} \in \mathbb{R}^N; \ |y_\ell^i| \leq a_\ell, \ \frac{1}{\delta} |y_\ell^{i+1} - y_\ell^i| \leq b_\ell; \ i = 0, \dots, n, \ \ell = 1, \dots, 6 \right\},$$

where we have set $N = 6(n+1)$.

We can now replace the constrained minimization problem (2.9) by the following finite dimensional minimization problem

Find $\boldsymbol{y}^* \in \mathcal{K}_\delta \subset \mathbb{R}^N$ such that :

$$E_{\delta h}(\boldsymbol{y}^*) \leq E_{\delta h}(\boldsymbol{y}), \quad \forall \boldsymbol{y} \in \mathcal{K}_\delta. \tag{3.6}$$

The set $\mathcal{K}_\delta$ is closed and bounded and therefore a compact subset of $\mathbb{R}^N$. Thus, according to the Weierstrass theorem, the problem (3.6) has at least one local minimum.

3.2 Computing the gradient of the cost function

The approximate cost functional $E_{\delta h}$ is a differentiable function and its gradient can be computed straight from (3.5). But we can take advantage of the optimal control structure of the problem. Indeed, y can be viewed as a control variable, and $u^n(x) = u(x; y^n)$ as a state variable and (3.1) the state equation. Let us rewrite (3.1) as

$$Q(x^j; y^n) = \sum_{i=0}^{n} w_i q(x^j; y^i), \quad j = 1, \ldots m, \tag{3.7}$$

where

$$w_i = \begin{cases} \delta/2 & \text{if } i \in \{0, n\}, \\ \delta & \text{if } i = 1, \ldots, n-1, \end{cases}$$

and m is the number of grid points in Ω. If we set $u_j^n = u^n(x^j)$, then the state equation (3.1) becomes

$$u_j^n - Q(x^j; y^n) = 0, \quad j = 1, \ldots, m.$$

The adjoint variable $p_j = p(x^j)$ is computed pointwise using the adjoint equation

$$p_j = -\frac{\partial E_{\delta h}(\boldsymbol{y})}{\partial u_j^n} = -\sum_{e \in V_j} \frac{|\Omega_e|}{4} \left(u_j^n - u^*(x^j) \right), \quad j = 1, \ldots, m, \tag{3.8}$$

where V_j is the index set of the parallelograms sharing the vertex x^j. Following the adjoint-state technique, since E does not depend explicitly on $\boldsymbol{y}$, we have

$$\frac{\partial E_{\delta h}(\boldsymbol{y})}{\partial y^k} = \frac{\partial E_{\delta h}(\boldsymbol{y})}{\partial y^k} + \sum_{j=1}^{m} \frac{\partial}{\partial y^k} \left(u_j^n - Q(x^j; y^n) \right) \cdot p_j$$

$$= \sum_{j=1}^{m} w_k \frac{\partial q(x^j; y^k)}{\partial y^k} \sum_{e \in V_j} \frac{|\Omega_e|}{4} \left(u_j^n - u^*(x^j) \right),$$

using (3.7) and (3.8).

3.3 An augmented Lagrangian method

Various algorithms for solving the nonlinear optimization problem (3.6) exist (see e.g. [2, 4, 7] and references therein). In this section, we focus on a solution method based on the augmented Lagrangian.

Since box constraints are easy to manage, let us introduce the set of box constraints K defined by

$$K = \left\{ \boldsymbol{y} \in \mathbb{R}^N; \ |y_\ell^i| \leq a_\ell, \ i = 0, \ldots, n, \ \ell = 1, \ldots, 6 \right\}.$$

The problem (3.6) is of the form

$$\min F(\boldsymbol{y}) \tag{3.9}$$

$$-b_j \leq h_j(\boldsymbol{y}) \leq b_j, \quad j = 1, \ldots, M, \tag{3.10}$$

$$\boldsymbol{y} \in K \subset \mathbb{R}^N, \tag{3.11}$$

where h_j denotes the jth two-sided constraint, on the derivative, in $\mathcal{K}_\delta$, $-b_j$ and b_j its lower and upper bound, respectively.

A way to overcome the constraints (3.10) is to associate to them Lagrange multipliers through a Lagrangian function. To avoid splitting each two-sided constraint in two inequality constraints and consequently two associated Lagrange multipliers, we use an augmented Lagrangian method for two-sided constraints due to [2]. The idea is to replace (3.9)-(3.11) by the following equivalent problem

$$\min F(\boldsymbol{y})$$
$$-b_j \leq h_j(\boldsymbol{y}) - v_j \leq b_j, \quad j = 1, \ldots, M$$
$$v_j = 0, \quad j = 1, \ldots, M,$$
$$\boldsymbol{y} \in K \subset \mathbb{R}^N.$$

Thus, we can construct the augmented Lagrangian with only the constraints $v_j = 0$ to obtain

$$\min \mathscr{L}(\boldsymbol{y}, \boldsymbol{\lambda}, \boldsymbol{r}) = F(\boldsymbol{y}) + \boldsymbol{\lambda}^T \boldsymbol{v} + \frac{1}{2} \sum_{j=1}^{M} r_j |v_j|^2 \tag{3.12}$$

$$-b_j \leq h_j(\boldsymbol{y}) - v_j \leq b_j, \quad j = 1, \ldots, M \tag{3.13}$$
$$\boldsymbol{y} \in K \subset \mathbb{R}^N, \tag{3.14}$$

where $\boldsymbol{\lambda} \in \mathbb{R}^M$ is the Lagrange multiplier vector and $\boldsymbol{r} = (r_j)$, $r_j > 0$, the vector of penalty parameters. The fictitious unknown $\boldsymbol{v}$ is eliminated by a straightforward calculation and the problem (3.12)-(3.14) becomes

$$\min \mathscr{L}(\boldsymbol{y}, \boldsymbol{\lambda}, \boldsymbol{r}) = F(\boldsymbol{y}) + \sum_{j=1}^{M} c_j(h_j(\boldsymbol{y}), \lambda_j, r_j) \tag{3.15}$$

$$\boldsymbol{y} \in K, \ \boldsymbol{\lambda} \in \mathbb{R}^M, \ \boldsymbol{r} > 0 \tag{3.16}$$

where c_j is defined by

$$c_j(h_j(\boldsymbol{y}), \lambda_j, r_j) = \begin{cases} \lambda_j (h_j(\boldsymbol{y}) - b_j) + \frac{r_j}{2} (h_j(\boldsymbol{y}) - b_j)^2 & \text{if } z(h_j(\boldsymbol{y}), \lambda_j, b_j) > 0 \\ \lambda_j (h_j(\boldsymbol{y}) + b_j) + \frac{r_j}{2} (h_j(\boldsymbol{y}) + b_j)^2 & \text{if } z(h_j(\boldsymbol{y}), \lambda_j, -b_j) < 0 \\ -\frac{\lambda_j^2}{2r_j} & \text{otherwise}, \end{cases}$$

with

$$z_j(h_j(\boldsymbol{y}), \lambda_j, \xi) = \lambda_j + r(h_j(\boldsymbol{y}) - \xi).$$

The problem (3.15)-(3.16) can be solved by the following augmented Lagrangian algorithm.

Algorithm AL

- $k \leftarrow 0$. Initialization
    $\lambda^0 \leftarrow 0$, $r_j > 0$, $0 < \beta < 1$ and $\gamma > 0$ given
- $k \geq 0$. Assuming $\boldsymbol{\lambda}^k$ and $\boldsymbol{r}^k$ are known, compute $\boldsymbol{y}^k$, $\boldsymbol{\lambda}^{k+1}$ and $\boldsymbol{r}^{k+1}$ as follows.

– Minimization step
Find $\boldsymbol{y}^k \in K$ such that

$$\mathscr{L}(\boldsymbol{y}^k, \boldsymbol{\lambda}^k, \boldsymbol{r}^k) \leq \mathcal{L}(\boldsymbol{y}, \boldsymbol{\lambda}^k, \boldsymbol{r}^k), \quad \forall \boldsymbol{y} \in K.$$

– Update Lagrange multipliers

$$\lambda_j^{k+1} = \begin{cases} \lambda_j^k + r_j^k(h_j(\boldsymbol{y}^k) - b_j) & \text{if } z(h_j(\boldsymbol{y}^k), \lambda_j^k, b_j) > 0 \\ \lambda_j^k + r_j^k(h_j(\boldsymbol{y}^k) - a_j) & \text{if } z(h_j(\boldsymbol{y}^k), \lambda_j^k, -b_j) < 0 \\ 0 \text{ otherwise,} \end{cases}$$

– Update the penalty parameters

$$r_j^{k+1} = \begin{cases} \beta r_j^k & \text{if } |c_j(h_j(\boldsymbol{y}^k), \lambda_j^k, r_j^k)| > \gamma|c_j(h_j(\boldsymbol{y}^{k-1}), \lambda_j^{k-1}, r_j^{k-1})| \\ r_j^k & \text{otherwise,} \end{cases}$$

We iterate until the constraints violation is sufficiently "small", i.e.

$$\sum_{j=1}^{M} c_j(h_j(\boldsymbol{y}^k), \lambda_j^k, r_j^k)^2 < \varepsilon^2. \tag{3.17}$$

4 Numerical experiments

In this paper, we are only interested in optimization within the main field body and not in the boundaries zones where more complex phenomena occur. A constant prescribed dose fixed at 80 Kg/Ha is considered because, although if in some cases desired application rates are constant, it is difficult to obtain an uniform deposit. The tractor speed is fixed at $V = 10$Km/h. We consider a field $\Omega = (0, 12\text{m}) \times (0, 100\text{m})$ with two tramlines
  – $s^1(t) = (0, Vt)$, $t \in (0, T)$, the outward path;
  – $s^2(t) = (12, 100 - V(t - T))$, $t \in (T, 2T)$, the return path.
The considered mechanical constraints are chosen in order to gather the characteristics of the most used spreaders. The selected bound constraints are presented in Table 1. The standard deviation parameters in (2.2) are $\sigma_r = 0.85$ and $\sigma_\theta = 19.3°$.

	Lower bound	Upper bound
Mass Flow Rate (Kg/min)	0	300
Medium Radius (m)	4	50
Medium Angle (°)	-80	80
Mass Flow Rate derivative (Kg/(min.s))	-0.5	0.5
Medium Radius derivative (m/s)	-3	3
Medium Angle derivative (°/s)	-6	6

TAB. 1 – Bound constraints

The time interval is (0, 46.8s), discretized with the time step $\delta = 46.8/260 = 0.18$s. The number of unknowns is therefore $12 \times 261 = 3132$. The space discretization is carried out by dividing Ω into squares of size 1m $\times$ 1m, i.e. 1313 grid points. The augmented Lagrangian algorithm is initialized with the following parameters : $\boldsymbol{r}^0 = 1$, $\gamma = 0.25$, $\beta = 10$ and $\boldsymbol{\lambda} = 0$. The starting solution is defined as follows

Left Disc : mass flow rate $= 8$, medium radius $= 9$, medium angle $= -15$;

Right Disc : mass flow rate $= 8$, medium radius $= 9$, medium angle $= 15$.

We use the Limited memory BFGS (L-BFGS, see e.g. [9]) for the unconstrained minimization step (Step 2. in Algorithm AL of Section 3.3). The stopping criteria are $\left\| \nabla_y \mathcal{L}(\boldsymbol{y}^k, \boldsymbol{\lambda}^k, \boldsymbol{r}^k) \right\| < 10^{-3}$ for L-BFGS and (3.17) with $\varepsilon = 10^{-5}$. All computations were carried out with Matlab software on a workstation (2.8 Ghz) running Windows XP.

With the above data (and after conversion in suitable units) Algorithm AL stopped after only one augmented Lagrangian iteration. In the L-BFGS routine, the convergence is reached after 389 iterations. As we can observed in Fig. 1, the application errors are less than 1% compared to the standard working application errors tolerance of 15%. The computed optimal parameters are shown in Fig. 2. They are relatively smooth and evolve around an average value that is very close to the starting solution. We can also notice some irregularities at the beginning at the end of the travel for the medium angle. These little discrepancies show that instantaneous variations are necessary when the spreader comes into the field and leave it.
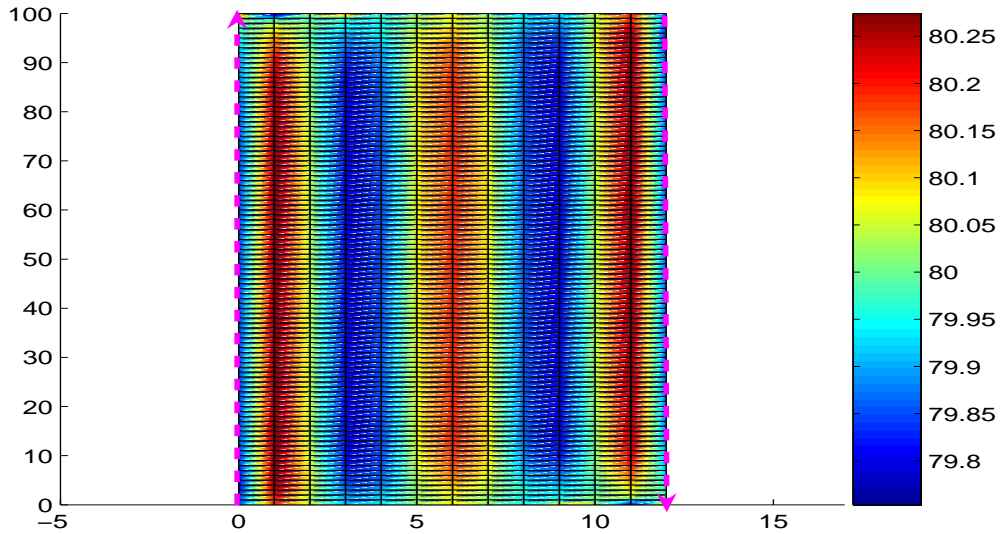

FIG. 1 – Computed dose map

5 Conclusion

We have proposed a new approach for the minimization of fertilizer application errors with centrifugal spreaders. An optimization criterion has been formalized from a spread pattern model studied in previous works. In order to take into account the mechanical limits of the spreaders, constraints have been considered. To handle efficiently these constraints, an augmented Lagrangian algorithm has been implemented within a Matlab environment. For a constant prescribed application rate, we have obtained satisfactory results. Furthermore, the optimal solution are very coherent with actual settings which would be done by agricultural engineers. These solutions can then be used in the future
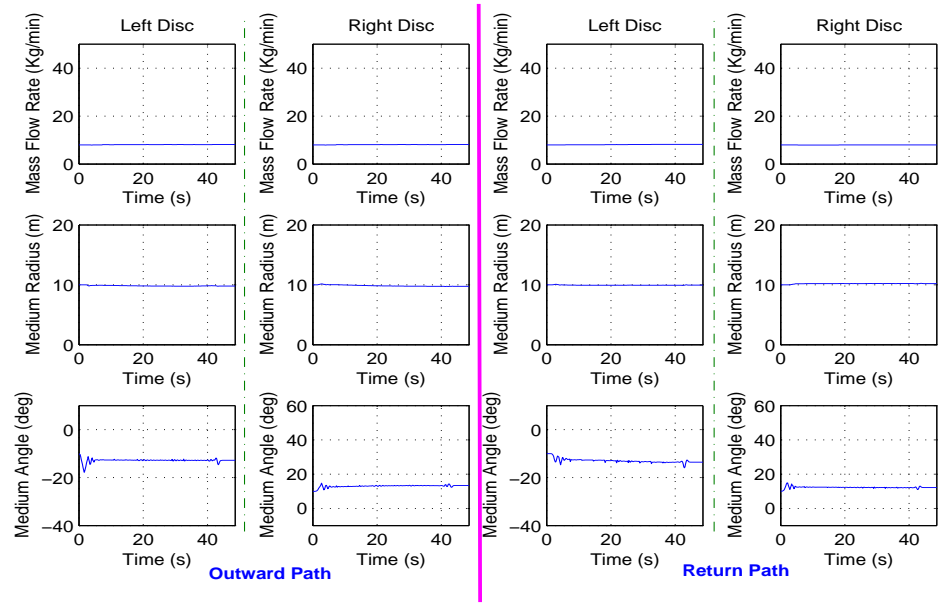
Fig. 2 – Computed optimal parameters

as reference variables to control centrifugal spreaders. Further study is underway to improve our model and algorithm (optimal control with a partial differential equation and parallelization).

Références

[1] ASAE, *S341.3 Procedure for Measuring Distribution Uniformity and Calibrating Granular Broadcast Spreaders.* 48th ed., St. Joseph, Michigan, USA, 2001.

[2] BERTSEKAS D.P., *Constrained Optimization and Lagrange Multipliers Methods*, Academic Press, 1982.

[3] COLIN A., *Etude du procédé d'épandage centrifuge d'engrais mineraux*, PhD thesis, Université Technologique de Compiègne, 1997.

[4] CONN A.R., GOULD N.I.M. and TOINT PH.L., Large-scale nonlinear constrained optimization : a current survey *Algorithms for continuous optimization : the state of the art*, Dordrecht, The Netherlands, pp. 287-332, 1994.

[5] DILLON C., SHEARER S., FULTON J. and KANAKASABAI M., Optimal path nutrient application using variable rate technology, *Proc. of the 4th European Conference on Precision Agriculture*, Berlin, Germany, pp. 171–176, 2003.

[6] FULTON J. P., SHEARER S. A., STOMBAUGH T. S., ANDERSON M. E., BURKS T. F. and HIGGINS S. F. (2003) : Simulation of fixed- and variable-rate application of granular materials, *Transactions of the ASAE*, Vol. 46, No. 5, pp. 1311–1321, 2003.

[7] GOULD N.I.M., Some reflections on the current state of active-set and interior point methods for constrained optimization, *SIAG/OPT Views-and-News*, Vol. 14, No. 1, pp. 2–7, 2003.

[8] ISO, (1985) : *ISO 5690/1 Equipment for distributing fertilizers - Test methods - Part 1 : Full width fertilizer distributors*, International Organization for Standardization, Genève, 1985.

[9] LIU D. C. and NOCEDAL J., On the limited memory BFGS method for large scale optimization, *Mathematical Programming*, Vol. 45, No. 3, pp. 503–528, 1989.

[10] OLIESLAGERS R., (1997) : *Fertilizer distribution modelling for centrifugal spreader design*, PhD thesis, K. U. Leuwen, Belgium, 1997.

[11] ROUSSELET M., COILLARD J. and MIRALLES A., *Les matériels de Fertilisation et Traitement des cultures*, Cemagref, Paris, 1997.

[12] YULE I., LAWRENCE H. and MURRAY R., Performance of fertiliser spreading equipment for precision agriculture applications, *Proceedings of 1st International Symposium on Centrifugal Fertiliser Spreading*, Leuwen, Belgium, pp. 10–18, 2005.